23rd ABCM International Congress of Mechanical Engineering
December 6-11, 2015, Rio de Janeiro, RJ, Brazil

COMPARISON BETWEEN FLUORESCENT CLASSIC 2D PIV AND FLUORESCENT STEREO-PIV MEASUREMENTS OF THE LIQUID PHASE VELOCITY IN A BUBBLE COLUMN

Rodrigo de Lima Amaral
University of Campinas, School of Chemical Engineering, Albert Einstein ave., 500 – Zip Code: 13083-852, Campinas-SP, Brazil.
rlamaral@feq.unicamp.br
Diana Isabel Sánchez Forero
University of Campinas, School of Chemical Engineering, Albert Einstein ave., 500 – Zip Code: 13083-852, Campinas-SP, Brazil.
sanchezd@feq.unicamp.br
Guilherme José de Castilho
University of Campinas, School of Chemical Engineering, Albert Einstein ave., 500 – Zip Code: 13083-852, Campinas-SP, Brazil.
guilhermejc@feq.unicamp.br
Sávio Souza Venâncio Vianna
University of Campinas, School of Chemical Engineering, Albert Einstein ave., 500 – Zip Code: 13083-852, Campinas-SP, Brazil.
savio@feq.unicamp.br
Milton Mori
University of Campinas, School of Chemical Engineering, Albert Einstein ave., 500 – Zip Code: 13083-852, Campinas-SP, Brazil.
mori@feq.unicamp.br

Abstract. *The Fluid dynamic analysis in bubble column reactors is important in heat and mass transfer and chemical reaction rate. Particle Image Velocimetry (PIV) is a non-intrusive technique used to determine the 2D (Classic 2D PIV) or 3D (Tomographic PIV) velocity field. Using the Stereoscopic –PIV (Stereo-PIV) it is possible to determine the third component of velocity by two cameras with different projections, resulting in a 3C-2D (two dimensional, three-component) field. The loss of correlation due to the out-of-plane motion of pairs of particle images, which is common in PIV applications, is reduced using the Stereo-PIV system. A problem encountered in Stereo-PIV applications is the restricted optical access in some facilities. Fluorescent tracer particles and a high-pass filter on the camera are used in Fluorescent PIV systems to determine the liquid phase velocity in bubble columns, so that the bubbles are not recorded in multiphase flow. This work aims to evaluate the quality of the Fluorescent Classic 2D PIV and Fluorescent Stereo-PIV measurements of the liquid phase velocity in a bubble column section. The Fluorescent Classic 2D PIV and Fluorescent Stereo-PIV images were processed using standard cross-correlation and ensemble correlation in order to compare the measurement quality. The cross-correlation coefficient, Signal-to-Noise Ratio (SNR) and PIV uncertainty estimated using correlation statistics were also analyzed as quality indicators.*

Keywords: *Fluorescent Stereo-PIV; Fluorescent Classic 2D PIV; PIV Correlation; Bubble Column, PIV uncertainty.*

1. INTRODUCTION

Most existing flows in industrial processes are completely 3D. Particle Image Velocimetry (PIV) is a non-intrusive technique often employed in determining the velocity field of multiphase flows. PIV technique can be classified depending on the component (C) and measurement domain (Dimension - D) of the velocity distribution: 2C-2D (Classic 2D PIV), 3C-2D (Stereo-PIV) and 3C-3D PIV (Tomographic-PIV). The PIV performance depends mainly on the concentration of tracer particles, particle image diameter, quality of the recorded images and processing. Classic 2D PIV uses one camera generally oriented at 90 degrees from the illuminated plane. The resulting 2C-2D vector field suffers from two deficiencies: (1) the out-of-plane velocity component is lost and (2) the measured in-plane components are themselves contaminated by perspective error. Stereoscopic imaging (Stereo-PIV) eliminates both the deficiencies above. Simultaneous views from two different off-axis directions provide sufficient information to extract the out-of-plane component as well as to correct errors in the in-plane components. A problem encountered in Stereo-PIV applications is the restricted optical access in some facilities allowing only the use of Classic 2D PIV (Prasad and Jensen, 1995; Prasad, 2000; Raffel *et al.,* 2007; Adrian and Westerweel, 2011).

A major problem of PIV applications in bubble columns is the large laser light scattering by the bubbles in relation to the tracer particles, which may damage the camera sensor. To avoid this problem, fluorescent tracer particles and a high-pass filter on the camera are used to allow only the passage of light scattered by the tracer particles. Even using a high-pass filter, usually recorded images present an unequal intensity distribution in the frame (complete image) interfering on the accuracy of the velocity distribution. This adapted technique is known as Fluorescent PIV (Northrup *et al.*, 1991; Linked and Merzkirch, 2002).

This work aims to evaluate the quality of Fluorescent Classic 2D PIV and Fluorescent Stereo-PIV measurements in a bubble column. The liquid phase velocity is analyzed by means of cross-correlation coefficient, Signal-to-Noise Ratio (SNR) and uncertainty estimated using correlation statistics. The Fluorescent Classic 2D PIV and Fluorescent Stereo-PIV images were processed using standard cross-correlation and ensemble correlation in order to compare the quality of the 2C-2D and 3C-2D measurements.

2. OUT-OF-PLANE MOTION

2.1 (3C-2D) Stereo-PIV

A major limitation in Classic 2D PIV systems is caused by the perspective error on the in-plane velocity components (Fig. 1a). This problem can be solved by using the Stereo-PIV (Fig. 1b). Stereo-PIV applies two cameras with different projections to record simultaneously the same field of view to determine the out-of-plane motion of the tracer particles providing a 3C-2D velocity field. The Scheimpflug condition (Fig. 1c) is used as a method to obtain images in good focus over the entire image plane. This condition requires that the object plane, lens plane, and image plane are colinear. The use of the Scheimpflug condition results in a significantly non-uniform magnification (di/do) across the image plane. The presence of out-of-plane particle motion or when the two laser sheets are not well overlapping change the relative intensity between particle images at first and second exposure. This difference of intensity was demonstrated to be the source of large errors (Raffel *et al.*, 2007; Nobach and Bodenschatz, 2009; Adrian and Westerweel, 2011).

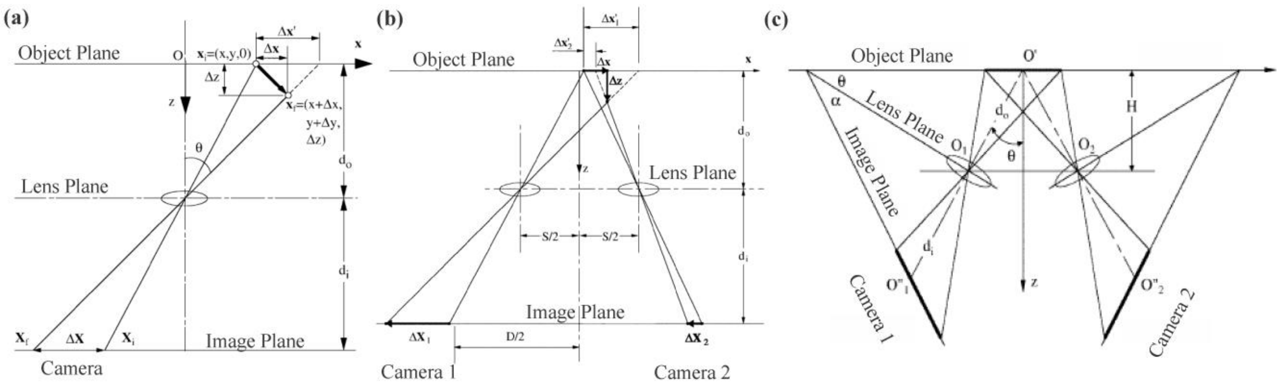

Figure 1 - (a) Measurement error due to the out-of-plane motion. (b) Stereoscopic imaging. (c) Scheimpflug condition (Adapted from Prasad, 2000)

2.2 Stereo Reconstruction

The essence of PIV image is to precisely measure the location of each particle (plane/object space) in the image plane in a calibration procedure (Fig 2a).

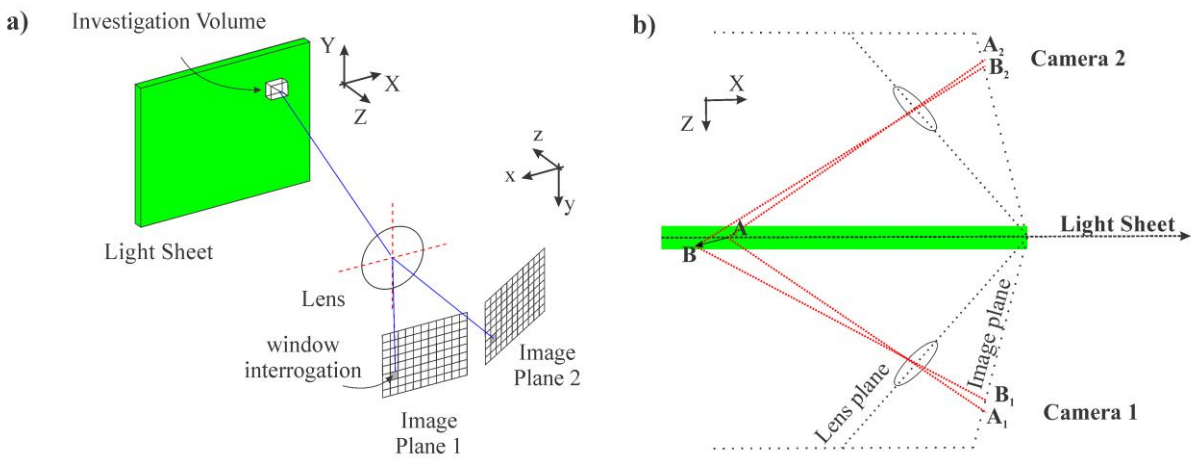

Figure 2 - Schematic representation of the Stereo-PIV (a) recording and (b) image.

The mapping should be an M function (known as mapping function) that relates the three-dimensional location of the particle in the fluid with two-dimensional space of the image plane. The inaccuracies in PIV calibration are caused by optical distortion due to inaccurate optical alignment, imperfection in lens design, refraction of optic windows, fluid interfaces and other optical elements in an experiment. In Stereo-PIV calibration, the mapping of two planes is needed for each camera, totaling two mapping functions per camera (Eq. 1). Projections of the velocity vectors on each camera, which correspond to the same real displacements, are associated. The third velocity component is obtained numerically with the matrices M_1 and M_2 of each camera (Soloff *et al*., 1997; Raffel *et al.*, 2007; Adrian and Westerweel, 2011).

$$\begin{pmatrix} x_{Ai} \\ y_{Ai} \\ 1 \end{pmatrix} = M_i \begin{pmatrix} X_A \\ Y_A \\ Z_A \\ 1 \end{pmatrix} \quad and \quad \begin{pmatrix} x_{Bi} \\ y_{Bi} \\ 1 \end{pmatrix} = M_i \begin{pmatrix} X_B \\ Y_B \\ Z_B \\ 1 \end{pmatrix} \quad i = 1, 2 \tag{1}$$

2C-2D velocity fields are determined by the motion of the particle image groups in small areas called interrogation windows by PIV correlation. This is known as PIV interrogation. Multiple passes decreasing the interrogation window size (multiple steps) are used to increase the Signal-to-Noise Ratio (SNR) in PIV interrogation. Usually, the 2C-2D vector fields have converged sufficiently after four passes at the final interrogation window size. The image dewarping and the image deformation are done simultaneously before each step in the multi-pass iterative scheme. The image dewarping is performed to compute the 2C-2D fields in the correct positions of the spatial coordinates. A sub-pixel interpolation is required during this process. The image deformation aims to compensate the distortion caused by the environment. The size and shape of the interrogation windows for both cameras are the same, that is, the correlation is done on the same particle images. A preliminary stereo reconstruction is done to remove the false vectors in the 2C–2D fields. Usually, these false vectors produce larger reconstruction errors (larger than 1 pixel). Then, the stereo reconstruction is performed solving a system of four linear equations with three unknowns (Vx, Vy, Vz). The deviation (reconstruction error) from the measured (Vx_{i1}, Vy_{i1}) and (Vx_{i2}, Vy_{i2}) reconstructed in image plane can be calculated from (Vx_1, Vy_1) and (Vx_2, Vy_2) components in 2C-2D vector field. Usually, the reconstruction error is below 0.5 pixels when the 2C vector error is less than 0.1 pixel. The reconstruction is accurate when the calibrated image is aligned with the object plane (illuminated plane) (Calluaud and David, 2004; Wieneke, 2005).

3. EXPERIMENTS

The experimental tests were carried out using the same acrylic bubble column investigated by Amaral *et al.* (2014) and Da Costa *et al.* (2014).

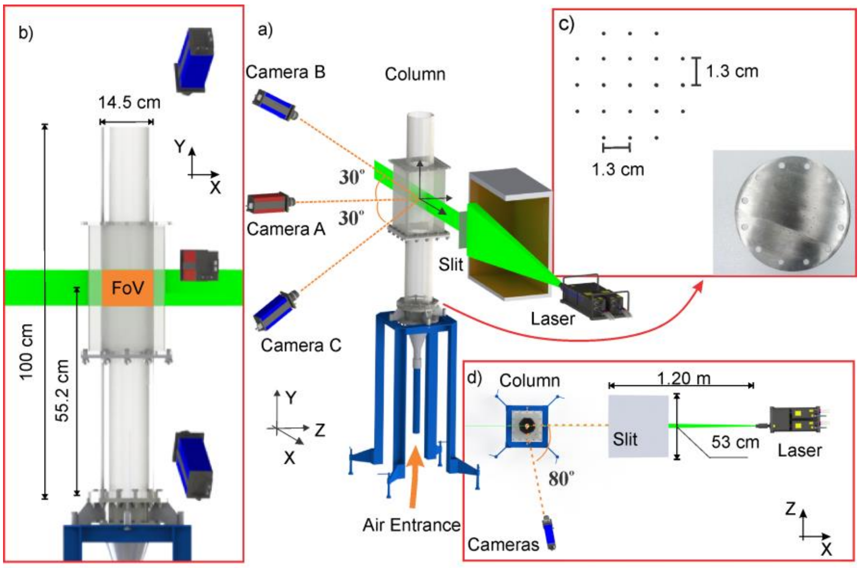

Figure 3 - (a) Bubble column, Fluorescent Classic 2D PIV (Camera A), Fluorescent Stereo-PIV (Camera B and C) and box with slit. (b) Field of View (FoV). (c) Air distributor with 21 holes. (d) PIV systems arrangement in the column.

Figure 3a shows the layout of the acrylic bubble column of 14.5 cm diameter and 1 m height. The column was filled with water at 25 °C and the gas phase used was air with a flow rate of 5, 20 and 40 L/min. The investigation area was located 55.2 cm from the distributor and had a size of 14.5 x 10 cm (Fig. 3b). A plane plate with 21 holes (1 mm in diameter) distributed equally in a square array (Fig. 3c) was used as a distributor. The Fluorescent Classic 2D PIV (Camera A) and Fluorescent Stereo-PIV (Camera B and C) are the same used by Amaral *et al.* (2014) and Da Costa *et al.* (2014), respectively. The Fluorescent PIV systems were developed by LaVision. The cameras (two CCDs with 1376 x 1040 pixels and 1376 x 1024 pixels) and the laser system (Nd:YAG, 200 mJ/pulse and λ = 532 nm) can be controlled with a programmable time unit (PTU) by Davis 8.2 software with a recording frequency of 5 Hz. The CCD cameras were placed at 80 degrees from the light plane in an angular configuration satisfying the Scheimpflug condition (Fig. 3d). An objective lens with focal distance of 60 mm (F/2.8D), Rhodamine-B as trace particle and a high-pass filter on the camera that allows only the passage of emitted light by tracer (λ = 620 nm) were used. The average resolution of the imaging system was 12 pixels/mm. 4000 pairs of images (Experiment 1 – Fluorescent Classic 2D PIV; Experiment 2 – Fluorescent Stereo-PIV) were recorded with a frequency of 4.2 Hz and the inter-frame time was 1000 µs, producing a particle image maximum displacement of 15 - 20 pixels.

In PIV preprocessing, RMS (Root Mean Square) and SSM (Subtract Sliding Minimum) filter of 3x3 pixels were applied sequentially in the recorded images. An upper limit of 50 counts and a pixel intensity lower than 10 counts were used in order to improve the image contrast. In PIV processing, the standard cross-correlation was made using an interrogation strategy with two steps: the first using an interrogation window size of 512 pixels (50% overlap of adjacent windows) and the second of 256 pixels (75% overlap of adjacent windows). The evaluation of multiple steps and Adaptive PIV method were used with decreasing interrogation window size in the PIV correlation. The Adaptive PIV method was used in order to change the size and shape of the interrogation window automatically according to the particle image density and flow gradients with the aim to increase the correlation coefficient and SNR. The initial and final size of the interrogation window was defined using 2 and 3 passes to ensure the convergence in determining the particle image displacement. The overlap of the interrogation window with its neighborhood was used in order to increase the spatial resolution of the vector field. For the image reconstruction were used the particle image displacement information of the first step and the mapping function using a bicubic interpolation (Fincham and Delerce, 2000; Scarano and Riethmuller, 2000). A Gaussian function was used for the peak detectability and the correlation peak was fitted by an estimator of three points (Westerweel, 1997).

The distributions of the time-averaged correlation coefficient, SNR and uncertainty estimated by Wieneke (2014, 2015) method were used as parameters of quality. The distributions of time-averaged velocity (modulus lVl; components Vx, Vy and Vz) were compared with the measurements obtained by the ensemble correlation (PIV sum of correlation) method (Meinhart *et al*., 2000). The ensemble correlation approach (PIV sum of correlation) is suitable to use when the SNR is very low. The disadvantage of this method is that it provides only the average field of a set of instantaneous obtained in the recording.

4. RESULTS AND DISCUSSIONS

Figure 4 shows the distribution of the time-averaged intensity across the radius (Y = 55,2 cm) in the Fluorescent Classic 2D PIV and Fluorescent Stereo-PIV frames for flow rates of 5, 20 and 40 L/min without PIV preprocessing. The intensity distribution is shown for the non-reconstructed images.

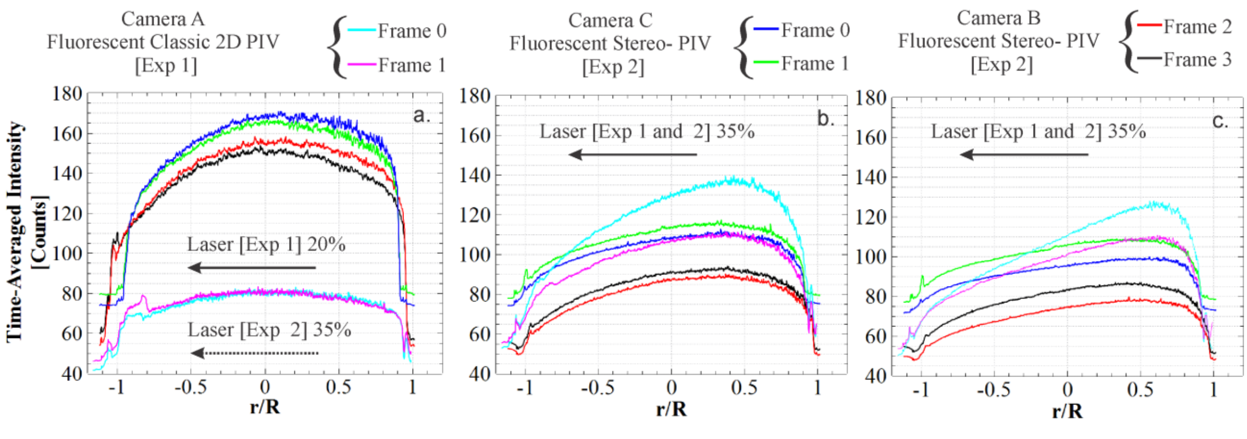

Figure 4 – Distribution of the time-averaged intensity across the radius (Y = 55,2 cm) in the Fluorescent Classic 2D PIV and Fluorescent Stereo-PIV frames for flow rates of (a) 5, (b) 20 and (c) 40 L/min without PIV preprocessing.

Besides the cameras with different projections, the bubbles cause an unequal distribution of intensity across the radius and between the frames of each camera (contributing to the backlighting). The light scattered on the column wall also contributes directly to the backlight.

Figure 5 shows the time-averaged lVl, Vx and Vy for the Fluorescent Classic 2D PIV and Fluorescent Stereo-PIV using the standard cross-correlation and ensemble correlation for flow rates of 5, 20 and 40 L/min. A small difference in the distribution of the time-averaged velocity (modulus and components) determined by the standard cross-correlation approach using the Fluorescent Classic 2D PIV and Fluorescent Stereo-PIV for flow rates of 5 and 20 L/min was observed in respect to the ensemble correlation. When using a flow rate of 40 L/min, a big difference can be observed by the Fluorescent Classic 2D PIV from r/R = 0 to -1. The velocities determined by the Fluorescent Stereo-PIV at 40 L/min using the standard cross-correlation are consistent with the values obtained using the ensemble correlation (for both techniques.).

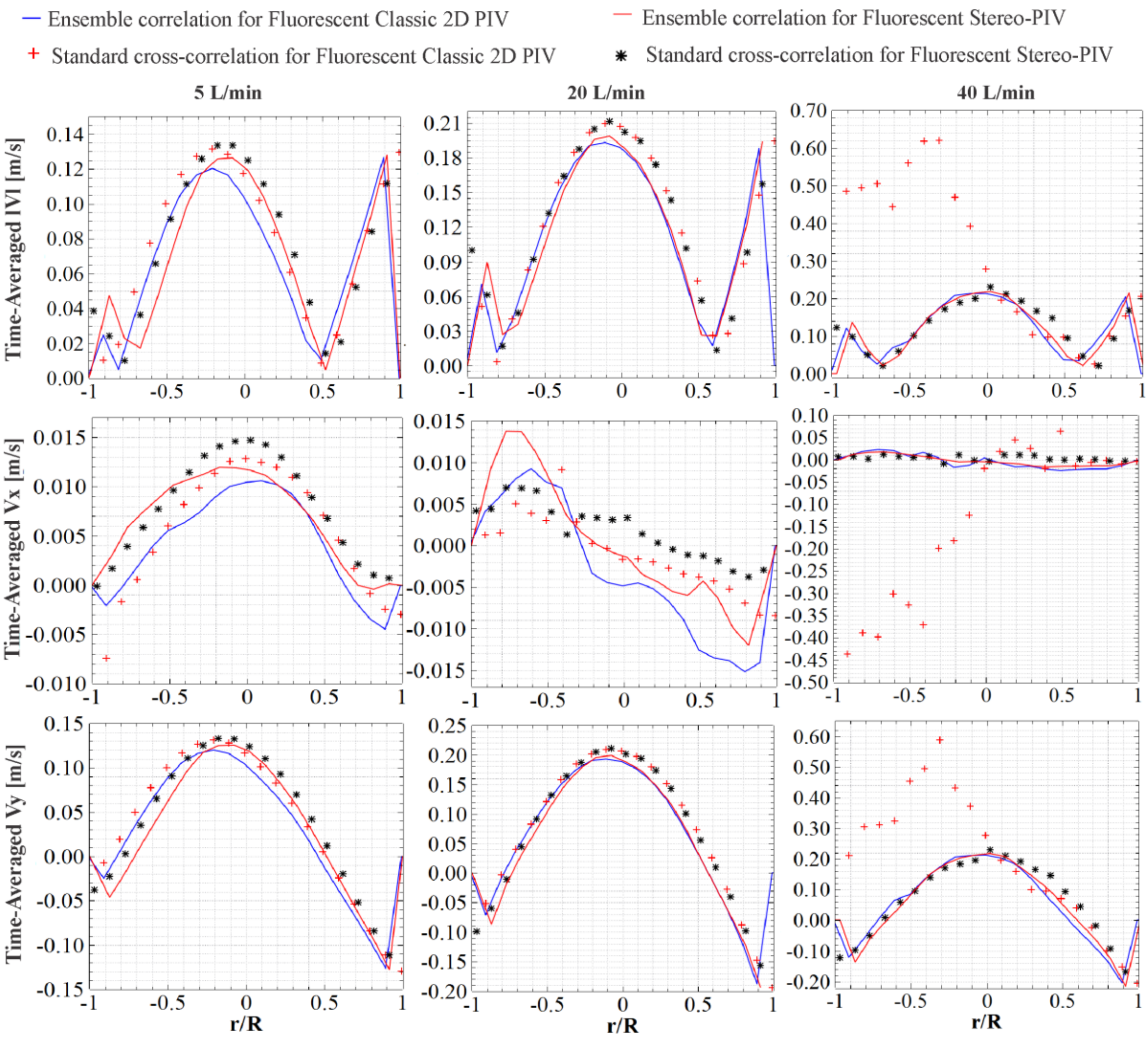

Figure 5 – Time-averaged lVl, Vx and Vy for the Fluorescent Classic 2D PIV and Fluorescent Stereo-PIV using the standard cross-correlation and ensemble correlation for flow rates of 5, 20 and 40 L/min.

When compared to the two correlation methods, the velocity values of the X component showed a lower consistency than the Y component for both techniques. This can be explained by the correlation peak detectability. Vy is greater than Vx (and Vz for the Fluorescent Stereo-PIV) due to the rise velocity of the bubbles. The particle image displacement in the Y direction is easier to identify than in the X direction (and Vz for the Fluorescent Stereo-PIV) for a selected time interval dt (1000 s). The asymmetric velocity profile in Fig. 5 can be caused by the recirculation regions in column or distributor design. It was also observed that the wall condition (lVl = Vx = Vy = Vz = 0) is not satisfied. This can be explained by the low spatial resolution of both techniques, which is not able to determine the small structures near the wall.

The profiles of the Z velocity component and stereo reconstruction error using the standard correlation and ensemble correlation method for different flows are shown in Fig. 6. Increasing the flow rate, a big difference between Vz using both correlation methods was observed. The stereo reconstruction error using the standard correlation was greater than the ensemble correlation. Increasing the flow rate, the reconstruction error increases using the standard correlation.

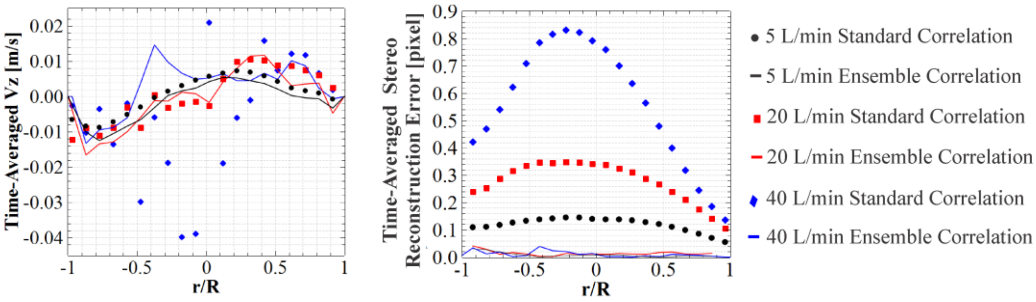

Figure 6 – Time-averaged of the Vz and Stereo Reconstruction error.

Time-Averaged of the cross-correlation coefficient and Signal-to-Noise Ratio (SNR) for the standard correlation method is presented in Fig. 7a and 7b. According Xue *et al.* (2013), numerical investigations show that a correlation coefficient of 0.5 and SNR of 2.0 are ideal to avoid errors in the vector field (red line in Fig. 7a and 7b).

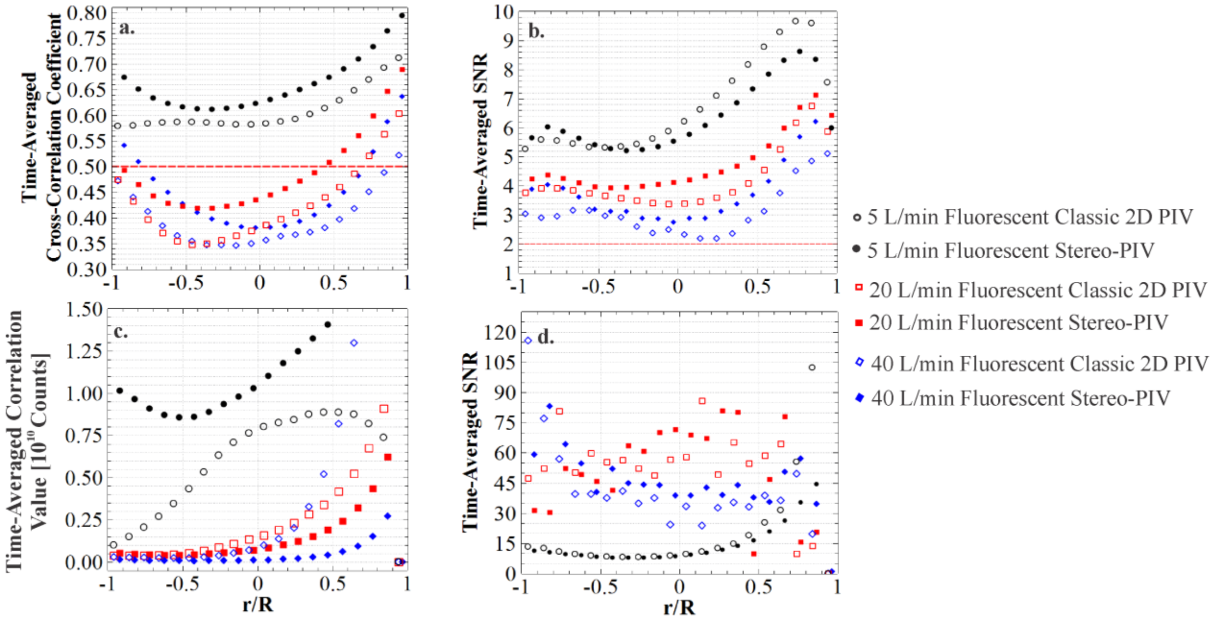

Figure 7 – Time-averaged of the (a) cross-correlation coefficient and (b) Signal-to-Noise Ratio (SNR) for the standard correlation method. Time-averaged of the (c) correlation value and (d) Signal-to-Noise Ratio (SNR) for the ensemble correlation method.

The time-averaged cross-correlation coefficient is higher for the Fluorescent Stereo-PIV than the Fluorescent Classic 2D PIV measurements (except at flow rate of 5 L/min). This can be attributed to the loss of correlation due to the out-of-plane motion of the particles. The cross-correlation coefficient and SNR decrease with increasing flow rate. In Fig 7c, the time-averaged correlation value is larger for the velocities calculated by the ensemble correlation in region from r/R = 0 to 1. This is directly related to the amount of particle images in the frame. In Fig. 7d it is observed that the SNR of the velocities calculated by the ensemble correlation is greater than the standard cross-correlation method. This shows that the correlation ensemble method is robust.

The uncertainty of the PIV measurements consists of the standard deviation (random errors) and bias (systematic errors). Each displacement vector is associated with a higher or lower error estimate (a bias error) and some degree of random errors or measurement uncertainty (Raffel *et al.*, 2007). The time-averaged of the bias and standard deviation is showed in Fig. 8 and 9 using the Wieneke (2014) method. Figure 8 shows that the standard deviation for the velocity components (Vx, Vy and Vz) increases with the flow rate. The Fluorescent Classic 2D PIV measurements showed greater uncertainty (except at 5 L/min) and lower bias than the Fluorescent Stereo-PIV measurements. The uncertainty in determining the time-averaged velocity by the Fluorescent Stereo-PIV in some regions is larger and can be explained by the uncertainty Vz (even with Vx and Vy lower than that determined by the Fluorescent Classic 2D PIV). This shows that the Fluorescent Stereo-PIV can be used primarily to determine Vx and Vy with a higher accuracy. However, the Fluorescent Classic 2D PIV measurements of the Y velocity component (axial direction in the bubble column) calculated by the ensemble correlation are acceptable in respect to the Fluorescent Stereo-PIV.

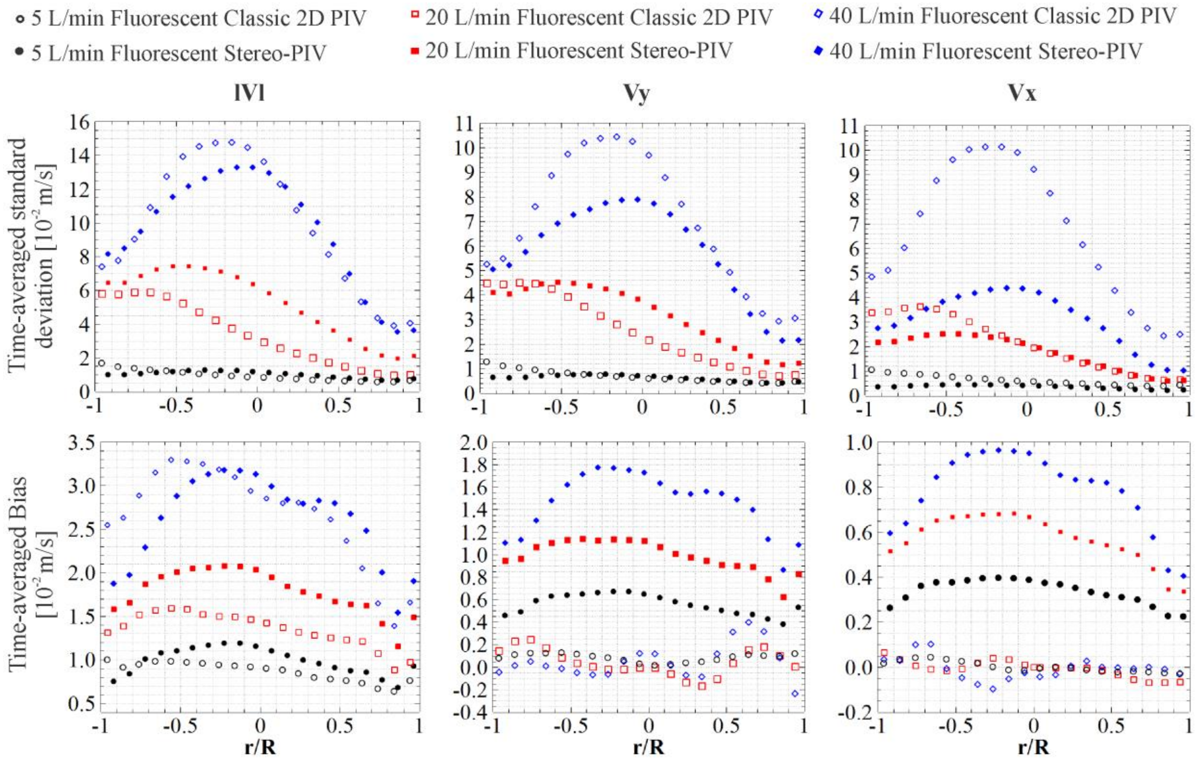

Figure 8 – Time-averaged of the Bias and Standard Deviation for lVl, Vx e Vy obtained by the Fluorescent Classic 2D PIV and Fluorescent Stereo-PIV.

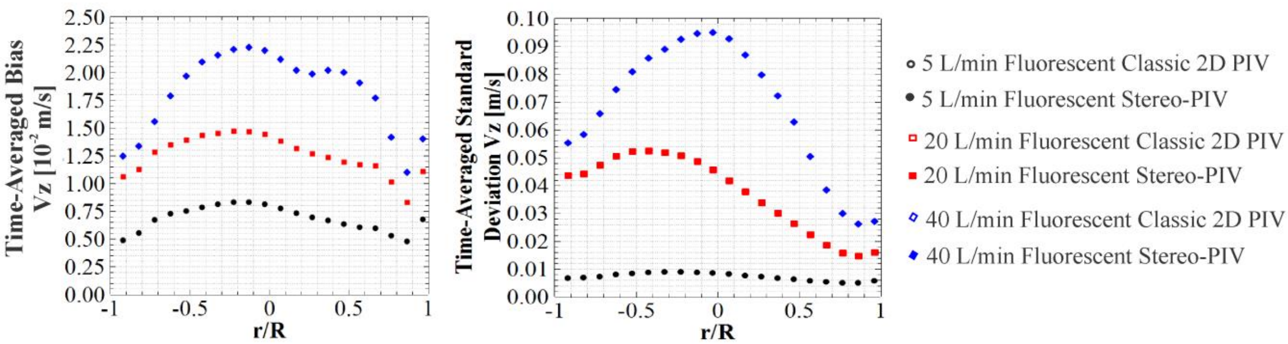

Figure 9 – Time-averaged of the Bias and Standard Deviation for Vz obtained by the Fluorescent Stereo-PIV.

5. CONCLUSION

This work evaluated the quality of the Fluorescent Classic 2D PIV and Fluorescent Stereo-PIV measurements on liquid phase velocity in a bubble column section analyzing the cross-correlation coefficient, Signal-to-Noise Ratio (SNR) and uncertainty by correlation statistics. The distributions of the time-averaged velocity (modulus lVl; components Vx, Vy and Vz) calculated by standard PIV cross-correlation were compared with the measurements obtained by the ensemble correlation (PIV sum of correlation) method. The ensemble correlation approach (PIV sum of correlation) is suitable to use when the SNR is very low. The disadvantage of this method is that it provides only the average field of a set of instantaneous data obtained in the recording. A major limitation in the Fluorescent Classic 2D PIV systems is caused by the perspective error on the velocity components in the plane. This problem can be solved by using the Fluorescent Stereo-PIV. However, a problem encountered in the Fluorescent Stereo-PIV applications is the restricted optical access in some facilities allowing only the use of the Fluorescent Classic 2D PIV. The distribution of the time-averaged intensity across the column radius recording in image frames for the both techniques was analyzed. Besides the cameras with different projections, the bubbles cause an unequal distribution of intensity across the radius and between the frames of each camera (contributing to the backlighting). A small difference in the distribution of the time-averaged velocity (modulus and components) determined by the standard cross-correlation approach using both techniques for flow rates of 5 and 20 L/min was observed in respect to the ensemble correlation. At flow rate of 40 L/min, a big difference was observed using the Fluorescent Classic 2D PIV from r/R = 0 to -1. The velocities determined by the Fluorescent Stereo-PIV at 40 L/min using the standard cross-correlation were consistent with the values obtained using the ensemble correlation for both techniques. When compared to the two correlation methods, the velocity values of the X component showed a lower consistency than the Y component for both techniques. This can be explained by the correlation peak detectability. The Y velocity component (axial direction, Vy) was greater than Vx (and Vz for the Fluorescent Stereo-PIV) due to the rise velocity of the bubbles. The particle image displacement in the Y direction is easier to identify than in the X direction (and Vz for the Fluorescent Stereo-PIV) for a selected time interval dt (1000 s). Increasing the flow rate, a big difference between Vz (out-of-plane component; radial direction) using the two correlation methods was observed. The stereo reconstruction error using the standard correlation was greater than the ensemble correlation. Increasing the flow rate, the reconstruction error increases using the standard correlation. The time-averaged cross-correlation coefficient was higher for the Fluorescent Stereo-PIV than the Fluorescent Classic 2D PIV measurements (except at flow rate of 5 L/min). This can be attributed to the loss of correlation due to the out-of-plane motion of the particles. The cross-correlation coefficient and SNR decreased with increasing flow rate. The Fluorescent Classic 2D PIV measurements showed greater uncertainty (except at 5 L/min) and lower bias than the Fluorescent Stereo-PIV measurements. The uncertainty in determining the time-averaged velocity by the Fluorescent Stereo-PIV in some regions is larger and can be explained by the uncertainty Vz (even with Vx and Vy lower than that determined by the Fluorescent Classic 2D PIV). This shows that the Fluorescent Stereo-PIV can be used primarily to determine Vx and Vy with a higher accuracy. However, the Fluorescent Classic 2D PIV measurements of the Y velocity component (axial direction in the bubble column) calculated by the ensemble correlation are acceptable in respect to the Fluorescent Stereo-PIV.

6. ACKNOWLEDGEMENTS

The authors would like to acknowledge Petrobras and Capes for the financial support of this project

7. REFERENCES

Amaral, R. L.; Forero D. I. S.; Da Costa. K. K.; Taranto, O. P.; Vianna, S. S. V.; Mori, M. Efeito da função de mapeamento na distribuição da velocidade da fase líquida na seção de uma coluna de bolhas por PIV. Congresso Brasileiro de Engenharia Química (COBEQ). Florianópolis-SC, Brasil, 2014.

Calluaud D. and David, L., 2004. Stereoscopic particle image velocimetry measurements of the flow around a surface-mounted block. Experiments in Fluids 36 p. 53–61.

Da Costa, K. K.; Forero, D. I. S.; Amaral, R. L.; Taranto, O. P.; Vianna, S. S. V.; Mori, M. Efeito da autocalibração para Stereo-PIV na distribuição da velocidade 2D3C da fase líquida em uma seção de uma coluna de bolhas. Congresso Brasileiro de Engenharia Química (COBEQ). Florianópolis-SC, Brasil, 2014.

Fincham, A. and Delerce, G., 2000. "Advanced optimization of correlation imaging velocimetry algorithms", Experiments in Fluids [Suppl.], Vol.29, p.13-22.

Meinhart, C. D., Wereley, S. T. and Santiago, J.G., 2000. A PIV Algorithm For Estimating Time-Averaged Velocity Fields, Journal of Fluids Engineering, Vol. 122, p. 285-289.

Nobach, H. and Bodenschatz, E., 2009. "Limitations of accuracy in PIV due to individual variations of particle image intensities". Exp Fluids. Vol. 47 pp 27–38.

Prasad, A. K. and Jensen, K., 1995. "Scheimpflug stereocamera for particle image velocimetry in liquid flows". Applied Optics. Vol. 34, No. 30

Prasad, A., 2000, "Particle image velocimetry - Review article", Current Science, Vol. 79, pp. 51-60.

Raffel, M.; Willert, C.; Wereley, S. T. and Kompenhans, J., 2007. Particle image velocimetry: a practical guide. Second Edi ed. Berlin Heidelberg: Springer Verlag.

Scarano, F. and Riethmuller, M.L., 2000. "Advances in iterative multigrid PIV image processing", Experiments in Fluids [Suppl.], Vol.29, p. 51-60.

Westerweel, J., 1997. "Fundamentals of digital particle image velocimetry", Meas. Sci. Technol. 8, p. 1379-1392.

Wieneke, B. and Pfeiffer, K., 2010. "Adaptive PIV with variable interrogation window size and shape", 15th Int Symp on Applications of Laser Techniques to Fluid Mechanics, Lisbon, Portugal.

Wieneke, B., 2005. Stereo-PIV using self-calibration on particle images, Experiments in Fluids,vol. 39, p. 267–280.

Wieneke, B., 2014. Generic a-posteriori uncertainty quantification for PIV vector fields by correlation statistics. 17th International Symposium on Applications of Laser Techniques to Fluid Mechanics, Lisbon, Portugal, 07-10 July.

Willert, C. E. and Gharib, M., 1991. 'Digital Particle Image Velocimetry', Experiments in Fluids, vol. 10, no. 4, p. 181-193.

8. RESPONSIBILITY NOTICE

The authors Rodrigo de Lima Amaral, Diana Isabel Sánchez Forero, Guilherme José de Castilho, Sávio Souza Venâncio Vianna and Milton Mori are the only responsible for the printed material included in this paper.